Proceedings of the 39th Chinese Control Conference
July 27-29, 2020, Shenyang, China

Standard Formation Generation and Keeping of Unmanned Aerial Vehicles Through a Potential Functional Approach

Huiming Li[1], Hao Chen[1], Shaowu Yang[2], Xiangke Wang[1]

1. College of Intelligence Science and Technology, National University of Defense Technology, Changsha 410073, P. R. China
E-mail: xkwang@nudt.edu.com

2. College of Computer Science and Technology, National University of Defense Technology, Changsha 410073, P. R. China

Abstract: This paper investigates the standard formation generation and keeping problem for multiple fixed-wing unmanned aerial vehicles (UAVs), where a standard formation is defined as the basic shape of UAVs when executing tasks. Firstly, a control law based on the gradient of potential functions is proposed to drive multiple UAVs to form and keep the standard formation, with theoretical analysis showing that the desired collective behaviors can be obtained. The control law is then extended to achieve obstacle avoidance by taking the virtual repulsion strategy into account. Numerical simulations are finally provided, verifying the effectiveness of the proposed strategy.

Key Words: Unmanned Aerial Vehicles, Potential Function, Obstacle Avoidance

1 Introduction

Motivated by the cooperative phenomena in animal groups, multi-agent systems has become a hot topic in the field of control and robotics community [1]. Formation control is one of the most active research directions in multi-agent systems. The objective of formation control is to enforce agents to form and keep some specific formation shapes in the process of completing tasks. For decades, as summarized in surveys [2, 3], different methods have been proposed to solve the formation control problem, such as the leader-follower method [4–6], the virtual structure method [7], the behavior-based method [8, 9], etc.

Different formation control methods have different properties. For leader-follower method, some agents are designed as leaders to move towards the destinations; other agents regard the leaders as reference points and follow the leaders. The leader-follower method is easy to implement, but the whole system can be affected by any failure of leaders. The virtual structure method takes the entire formation as a rigid body and maintains the rigid geometric relationship among each agent during movement. Consequently, it is hard to change the formation shape dynamically. For behavior-based method, several basic behaviors are prescribed for each agent, such as obstacle avoidance, formation keeping and goal seeking. The control action is decided from a weighted average of these behaviors. Thus, it is difficult to analyse the stability of the whole system.

Among all of these formation control methods, the potential function is widely used for its clear and straightforward idea [10–12]. The potential function determines the attractive-repulsive effect on agents, which includes two elements: (i) attraction to neighbors that are far away; (ii) repulsion from neighbors that are too close. Therefore, potential functions drive agents to converge to the desired states with minimum energy. In fact, the potential function occupies a large proportion in theoretical analysis and practical applications. In 1986, Khatib first applied the potential function method to obstacle avoidance [13]. Nowadays, it has become a classical method to design formation controller while achieving obstacle avoidance.

The artificial physics introduced in [14] is a method to define potential functions by simulating real physical force, which is also used to study the multi-agent formation control problem. In [15, 16], the artificial physics method has been proposed to study the standard formation generation problem of quadrotors, and the gradient descent control strategy is applied to agents with second-order integral model. Different from quadrotors, fixed-wing UAVs have some unique kinematic characteristics, which brings many challenges to their formation control problem [17, 18]. To be more precise, the motion of a fixed-wing UAV on a plane can be described by a unicycle model with input constraints, which is quite different from the quadrotor model employed in [15, 16].

In this work, we extend the formation control strategy proposed in [15, 16] to solve the problem of standard formation generation and keeping of multiple fixed-wing UAVs, and propose the virtual repulsion strategy to achieve obstacle avoidance. The main contributions of this work are summarized as follows. Firstly, we propose a novel distributed control law based on the gradient of a potential function, which drives UAVs to form and keep the standard formation. We theoretically prove that the desired collective behaviors can be obtained with the proposed control law. Secondly, we apply a novel virtual repulsion between UAVs and obstacles, so that the whole formation can change its own geometrical shape to avoid obstacles easily.

The paper is organized as follows. Section 2 presents the preliminary results and problem description. In Section 3, we design controllers to generate and keep the standard formation, while avoiding obstacles. Simulation results are shown in Section 4, and finally the concluding remarks are given in Section 5.

2 Problem Description

Consider a team of n fixed-wing UAVs flying at the same altitude, the position of the i-th UAV ($1 \leq i \leq n$) is denoted by the vector $p_i = [x_i, y_i]^T$ defined in an inertia coordinate frame $\mathscr{W}$ and θ_i is the UAV's heading angle with respect to the x-axis of $\mathscr{W}$. The kinematic equations of the i-th UAV

This work is supported by National Natural Science Foundation (NNSF) of China under Grant 61973309.

are described as

$$\begin{cases} \dot{x}_i = v_i \cos\theta_i \\ \dot{y}_i = v_i \sin\theta_i \\ \dot{\theta}_i = \omega_i \end{cases} \tag{1}$$

The control inputs of UAV_i are the linear speed v_i and angular speed ω_i. In practice, the maneuverability of fixed-wing UAVs limits the achievable v_i and ω_i, which can be described as input constraints

$$0 < v_{\min} \le v_i \le v_{\max}, \quad |\, \omega_i \,| \le \omega_{\max} \tag{2}$$

where $v_{\min}$ and $v_{\max}$ are the linear speed bounds of fixed-wing UAVs, and $\omega_{\max}$ is the maximum angular speed.

Remark 1 *In [15, 16], the second-order integrator model is used, which is much easier than the dynamics considered in* (1).

The communication network in a multi-agent system is usually modeled by an undirected graph $\mathcal{G} = \{\mathcal{V}, \mathcal{E}\}$, where $\mathcal{V} = \{1, 2, \ldots, n\}$ is a set of vertexes or nodes, and $\mathcal{E} \subseteq \mathcal{V} \times \mathcal{V}$ is the set of undirected edges. Let $\mathcal{N}_i$ denotes the set of the neighboring nodes of agent i, i.e., $\mathcal{N}_i = \{j \in \mathcal{V} : (i, j) \in \mathcal{E}\}$. To reduce interaction among UAVs, each UAV only has two neighbors, and the communication topology is organized in a *ring* form, as shown in Fig. 1.

Generally, the UAVs form some special shapes when executing the task, such as a line, a circle or a herringbone, etc. Inspired by the circular shape of the formation, we introduce the definition of *standard formation* [16], which can be seen as the fundamental formation of a multi-UAV system.

Definition 1 (Standard Formation [16]) *If all the UAVs are evenly distributed on the circle of radius R, and each UAV maintains a constant distance L from its neighbors, i.e.,*

$$\|p_i - p_c\| = R,\ \|p_i - p_j\| = L,\ j \in \mathcal{N}_i$$

where $p_c = [x_c,\ y_c]^T$ denotes the center of the circle, then such a formation shape is termed standard formation*.*

Remark 2 *As indicated in [16], the control law designed for the standard formation can be easily applied for the other formation shapes by using bijective transformation, provided that any three UAVs are not in the same line in the desired formation shape. In this paper, we only target at designing control law for the standard formation.*

According to Definition 1, in a standard formation, the UAVs are expected to form a regular polygon. The standard formation of six UAVs is shown in Fig.1.

Obviously, the relationship between the radius R and the distance L can be represented as

$$R = \frac{L}{2\sin(\frac{\pi}{n})}$$

We use p_{id} to represent the desired relative position of UAV_i in the standard formation. To make the standard formation unique, we pre-determine the position of UAV_1 on the circle as $p_{1d} = p^* = [x^*,\ y^*]^T$. Thus, the desired position of UAV_i can be calculated as

$$\begin{aligned} p_{id} &= [x_{id},\ y_{id}]^T \\ &= p_c + [R\cos(\alpha - (i-1)\beta),\ R\sin(\alpha - (i-1)\beta)]^T \end{aligned}$$

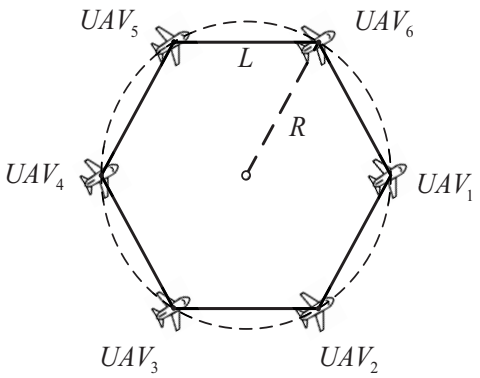

Fig. 1: An example of standard formation with six UAVs. All the UAVs are evenly distributed on the circle, and the communication topology is organized in a *ring* form.

where $\alpha = \arctan(\frac{y^* - y_c}{x^* - x_c})$, $\beta = \frac{2\pi}{n}$. Choose $y^* = y_c$ to simplify calculations. Therefore, the position of each UAV in the standard formation is calculated uniquely.

To form the unique standard formation and maintain the motion capability, we apply the leader-follower control strategy and put a virtual leader at the center of the unique standard formation with linear velocity v_d, and heading angle θ_d. A group of n fixed-wing UAVs exchange information over an undirected graph $\mathcal{G} = \{\mathcal{V}, \mathcal{E}\}$. All the actual UAVs act as the followers to track the virtual leader. The control objective includes two aspects: (i) the UAVs form the standard formation during the flight; (ii) the UAVs move at the same speed and towards the same direction with their virtual leader.

Assumption 1 *The virtual leader described by* (1) *moves along a straight line at constant speed. The speed v_d and heading angle θ_d are globally known to the followers. To guarantee all the UAVs can successfully track their virtual leader, it is necessary that $v_d \in [v_{\min}, v_{\max}]$.*

Now we can formulate the standard formation generation and keeping problem for fixed-wing UAVs as follows.

Problem: Given a team of n fixed-wing UAVs, each of which is modeled by (1), design control law $\mu = (v_i, \omega_i)$ such that $p_i \to p_{id}$, $v_i \to v_d$, $\theta_i \to \theta_d$.

3 Main Results

To achieve the above objective, we first design the formation control law to generate and keep the unique standard formation. Then, we extend the control law to meet the requirements of obstacle avoidance.

3.1 Formation Control Law Design

In this section, we discuss how to control the UAVs to achieve the desired collective motion.

First, to make UAVs converge to the standard formation, we define a potential function to measure the deviation of UAV_i's current position from its desired position:

$$\begin{aligned} F_i = \sum_{j \in \mathcal{N}_i} & \frac{1}{2} G(\|p_i - p_j\| - L)^2 + \\ & \frac{1}{2} G(\|p_i - p_c\| - R)^2 + \frac{1}{2}\|p_i - p_{id}\|^2 \end{aligned} \tag{3}$$

where G is a positive constant used to adjust the control effect, and p_c is the formation center. The first term in (3) measures the deviation of the UAV with respect to its neighbor, the second term measure the deviation of the UAV with respect to the formation center, and the third term is designed to guarantee the uniqueness of the standard formation. The potential function achieves local minimum at the unique standard formation, and the minimum value of the potential function is zero. The gradient of the function F_i, defined as a potential force, can be calculated as:

$$\begin{aligned} f_i =& \nabla_{p_i} F_i \\ =& \sum_{j\in\mathcal{N}_i} G(\|p_i-p_j\|-L)\frac{p_i-p_j}{\|p_i-p_j\|}+ \\ & G(\|p_i-p_c\|-R)\frac{p_i-p_c}{\|p_i-p_c\|}+(p_i-p_{id}) \end{aligned} \tag{4}$$

To drive UAVs to track the virtual leader, we define a speed force, f_v,

$$f_v = v_d[\cos\theta_d, \sin\theta_d]^T \tag{5}$$

Let $h_d = [\cos\theta_d, \sin\theta_d]^T$, $h_i = [\cos\theta_i, \sin\theta_i]^T$, $h_i^\perp = [-\sin\theta_i, \cos\theta_i]^T$. Then, $h_i^\perp h_i^{\perp T} = \boldsymbol{I} - h_i h_i^T$, where $\boldsymbol{I}$ is a identity matrix.

Finally, the formation control law is designed as

$$\begin{aligned} v_i &= [\cos\theta_i \ \sin\theta_i](-f_i+f_v) \\ &= -h_i^T f_i + v_d h_i^T h_d \\ \omega_i &= [-\sin\theta_i \ \cos\theta_i](-f_i+f_v) \\ &= -h_i^{\perp T} f_i + v_d h_i^{\perp T} h_d \end{aligned} \tag{6}$$

Remark 3 *The potential force defined in* (4) *contains three items. The first two items actually represent three forces that constrain each other, which determine the relative position of the i-th UAV in the formation. These three forces are easy to reach equilibrium, and the whole formation may fall into the local optimal solution. However, the desired position p_{id} in the third item is calculated according to the parameters of the first two terms, R and L, which determines a unique solution for the balance of forces. The third item provides a powerful extra force to avoid falling into the local extremum. Therefore, f_i can drive UAVs to the desired positions and form a predefined formation.*

Theorem 1 *Under Assumption 1, by applying control law (6), as $t\to\infty$, the following results hold: $p_i \to p_{id}$, $\|p_i - p_j\| \to L$, $\|p_i - p_c\| \to R$, $v_i \to v_d$, and $\theta_i \to \theta_d$.*

Proof Consider the Lyapunov function candidate

$$\begin{aligned} V =& \sum_{i=1}[\sum_{j\in\mathcal{N}_i}\frac{1}{4}G(\|p_i-p_j\|-L)^2+ \\ & \frac{1}{2}G(\|p_i-p_c\|-R)^2+\frac{1}{2}\|p_i-p_{id}\|^2 \\ & + v_d(1-\cos(e_{\theta_i}))]; \end{aligned} \tag{7}$$

Obviously, $V \geq 0$. The time derivative of the function V along the trajectories of (1) under the control law (6) is given by

$$\begin{aligned} \dot{V} =& \sum_{i=1}[\sum_{j\in\mathcal{N}_i}\frac{1}{2}G(\|p_i-p_j\|-L)\frac{(p_i-p_j)^T}{\|p_i-p_j\|}(\dot{p}_i-\dot{p}_j) \\ & + G(\|p_i-p_c\|-R)\frac{(p_i-p_c)^T}{\|p_i-p_c\|}(\dot{p}_i-\dot{p}_c) \\ & + (p_i-p_{id})^T(\dot{p}_i-\dot{p}_{id}) \\ & + v_d\sin(\theta_i-\theta_d)(\dot{\theta}_i-\dot{\theta}_d)] \end{aligned} \tag{8}$$

On the basis of the symmetry of the undirected graph $\mathcal{G}$, the equation (9) can be established

$$\begin{aligned} & \sum_{i=1}^{N}\sum_{j\in\mathcal{N}_i}(x_i-x_j)(\dot{x}_i-\dot{x}_j) \\ =& \sum_{i=1}^{N}\sum_{j\in\mathcal{N}_i}(x_i-x_j)\dot{x}_i - \sum_{i=1}^{N}\sum_{j\in\mathcal{N}_i}(x_i-x_j)\dot{x}_j \\ =& \sum_{i=1}^{N}\sum_{j\in\mathcal{N}_i}(x_i-x_j)\dot{x}_i + \sum_{j=1}^{N}\sum_{i\in\mathcal{N}_j}(x_i-x_j)\dot{x}_i \\ =& 2\sum_{i=1}^{N}\sum_{j\in\mathcal{N}_i}(x_i-x_j)\dot{x}_i \end{aligned} \tag{9}$$

So, equation (8) can be rearranged to obtain

$$\begin{aligned} \dot{V} =& \sum_{i=1}[f_i^T\dot{p}_i - G(\|p_i-p_c\|-R)\frac{(p_i-p_c)^T}{\|p_i-p_c\|}\dot{p}_c \\ & - (p_i-p_{id})^T\dot{p}_{id} + v_d\sin(\theta_i-\theta_d)(\dot{\theta}_i-\dot{\theta}_d)] \\ =& \sum_{i=1}[f_i^T h_i v_i - (p_i-p_{id})^T v_d h_d - v_d h_i^{\perp T} h_d \omega_i \\ & - G(\|p_i-p_c\|-R)\frac{(p_i-p_c)^T}{\|p_i-p_c\|}v_d h_d] \\ =& \sum_{i=1}[-f_i^T h_i h_i^T f_i - (v_d h_i^{\perp T} h_d)^2 \\ & + v_d f_i^T h_i h_i^T h_d + v_d h_i^{\perp T} h_d h_i^{\perp T} f_i \\ & - G(\|p_i-p_c\|-R)\frac{(p_i-p_c)^T}{\|p_i-p_c\|}v_d h_d \\ & - (p_i-p_{id})^T v_d h_d] \end{aligned} \tag{10}$$

where, some polynomials can be simplified as

$$\begin{aligned} & v_d f_i^T h_i h_i^T h_d + v_d h_i^{\perp T} h_d h_i^{\perp T} f_i \\ =& v_d f_i^T h_i h_i^T h_d + v_d f_i^T h_i^\perp h_i^{\perp T} h_d \\ =& v_d f_i^T h_d \end{aligned}$$

Thus, the equation (10) can be rewritten as

$$\begin{aligned}\dot{V} =& \sum_{i=1}[-f_i^T h_i h_i^T f_i - (v_d h_i^{\perp T} h_d)^2] + \\ & \sum_{i=1}[v_d f_i^T h_i h_i^T h_d + v_d h_i^{\perp T} h_d h_i^{\perp T} f_i \\ & - G(\|p_i - p_c\| - R)\frac{(p_i - p_c)^T}{\|p_i - p_c\|} v_d h_d \\ & - (p_i - p_{id})^T v_d h_d] \\ =& \sum_{i=1}[-f_i^T h_i h_i^T f_i - (v_d h_i^{\perp T} h_d)^2] + \\ & \sum_{i=1}[\sum_{j\in\mathcal{N}_i} G(\|p_i - p_j\| - L)\frac{(p_i - p_j)^T}{\|p_i - p_j\|} v_d h_d] \\ =& \sum_{i=1}[-f_i^T h_i h_i^T f_i - (v_d h_i^{\perp T} h_d)^2] \leq 0\end{aligned}$$

which implies that the system is stable. Since $\dot{V} = 0$ holds, we have that $f_i^T h_i h_i^T f_i = 0$ and $(v_d h_i^{\perp T} h_d) = 0$, which means $h_i^T f_i = 0$ and $\sin(\theta_i - \theta_d) = 0$.

As mentioned in LaSalle's invariance principle, any system starting from the initial positions converges to the largest invariant set of $h_i^T f_i = 0, e_{\theta_i} \in \{0, \pi\}$ over time. Thus, one of the following cases must hold:

(i) $f_i = 0$;
(ii) $f_i \neq 0$, but $h_i^T f_i = 0$.

For case (i), it is clear that the standard formation is an invariant set and the UAVs achieve the desired formation. More importantly, we now prove the case (ii) cannot establish. In this case, $h_i^T f_i = 0$ and $f_i \neq 0$ imply $f_i \perp h_i$. We can obtain the dynamics by replacing (6) in (1)

$$\begin{aligned}\dot{p}_i =& h_i v_i \\ =& h_i(-h_i^T f_i + v_d h_i^T h_d) \\ =& -h_i h_i^T f_i + v_d h_d - v_d h_i^{\perp} h_i^{\perp T} h_d \\ =& v_d h_d\end{aligned}$$

which means UAV_i's position is independent of the gradient f_i. In other words, UAV_i follows the leader and moves in a straight line. However,

$$\begin{aligned}\dot{h}_i =& h_i^{\perp} h_i^{\perp T}(-f_i + v_d h_d) \\ =& -f_i + h_i h_i^T f_i \\ =& -f_i \neq 0\end{aligned}$$

which implies the vector h_i is rotating. It is contradict with the truth $\dot{p}_i = v_d h_d$. Therefore, that case (ii) cannot happen. Thus, the desired formation is achieved, i.e., $p_i \to p_{id}$, $\|p_i - p_j\| \to L$, $\|p_i - p_c\| \to R$. By the way, $p_i \to p_{id}$ implies $v_i \to v_d$.

$\theta_i - \theta_d = 0$ or $\theta_i - \theta_d = \pi$ is derived from $\sin(\theta_i - \theta_d) = 0$. As proved above, the UAVs can achieve the standard formation so that $f_i = 0$, which means $v_i = v_d \cos(\theta_i - \theta_d)$. If $\theta_i - \theta_d = \pi$, we conclude $v_i = -v_d < 0$. This is a contradiction with the input constraints (2). Therefore, $\theta_i - \theta_d = 0$ is the only possible solution. As a result, all the UAVs follow the virtual leader with the same speed towards the same direction. ■

Remark 4 *Collision avoidance between UAVs and their neighbors depends on the potential function related to the relative distance, that is,* $\frac{1}{2}G(\|p_i - p_j\| - L)^2$. *When two UAVs get closer, the potential function increases, and behaves as a repulsion between the UAVs. Hence, the collision avoidance can be adjusted by the coefficient* G. *However, collision in general cannot be prevented between UAVs that are not adjacent because their relative distance does not affect the potential function. But it is effective to avoid collision during flight by selecting an appropriate threshold.*

The limited input is a difficult problem in the formation control of fixed-wing UAVs. In this paper, to meet the speed constraints (2), define a saturation function $\mathrm{sat}(x, a, b)$ to extend the control law (6). Suppose $a < b$, the saturation function is defined as

$$\mathrm{sat}(x, a, b) = \begin{cases} a, & x < a \\ x, & a \leq x \leq b \\ b, & x > b \end{cases} \tag{11}$$

Therefore, the proposed control law (6) can be rewritten as

$$\begin{aligned} v_i &= \mathrm{sat}\{h_i^T(-f_i + v_d h_d), v_{\min}, v_{\max}\} \\ \omega_i &= \mathrm{sat}\{h_i^{\perp T}(-f_i + v_d h_d), -\omega_{\max}, \omega_{\max}\} \end{aligned} \tag{12}$$

Remark 5 *The extended control law* (12) *can meet the input constraints of fixed-wing UAVs, and it is validated by simulations to drive UAVs to achieve the desired formation. It is worth future research to show the stability of the control law under input constraints.*

3.2 Obstacle Avoidance

As indicated in Remark 4, the collision avoidance mechanism between adjacent UAVs can be regarded as a repulsion force taking effect. Inspired by this idea, we apply the virtual repulsion strategy to achieve obstacle avoidance during the flight.

Regardless of the shapes of different obstacles, we describe an obstacle as a circle with radius of R_{obs}, where $p_{obs} = [x_{obs}, y_{obs}]^T$ denotes the centroid of the obstacle. If the distance between the UAV and the obstacle, $d_{obs} = \|p_{obs} - p_i\|$, is less than L_{obs}, the UAV will be subjected to a virtual repulsion f_{obs}, as shown in Fig.2.

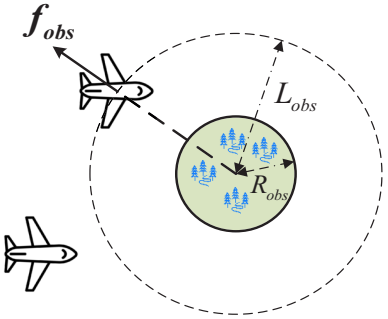

Fig. 2: Illustration of avoiding an obstacle using the virtual repulsion strategy.

The virtual repulsion f_{obs} is defined as,

$$f_{obs} = \begin{cases} \mathbf{0}, & d_{obs} > L_{obs} \\ k\frac{L_{obs} - d_{obs}}{d_{obs} - R_{obs}}\frac{p_i - p_{obs}}{\|p_i - p_{obs}\|}, & d_{obs} \leq L_{obs} \end{cases} \tag{13}$$

where k is a positive constant to adjust the repulsion. The greater the value of k, the lower the possibility of the UAV crashing the obstacle. If the UAV can make a quick turn, a small k is acceptable. R_{obs} is a parameter describing the size of the obstacle. L_{obs} is the braking distance, which is related to the cruise speed and acceleration of the UAV. According to (13), the larger d_{obs}, the smaller the virtual repulsion. Therefore, the UAV is subject to two forces, f_i and f_{obs}. The combined force enables the UAV to avoid crashing obstacles while keeping a standard formation.

4 Simulation

In this section, we present numerical simulations to verify the effectiveness of the proposed control law (6) and the virtual repulsion strategy. The formation control problem of six fixed-wing UAVs is considered, and the standard formation is shown in Fig. 1 with $L = 40m$. Thus, $R = L = 40m$ after calculation. The parameters of the virtual leader is set as $v_d = 15m/s$, $\theta_d = 0$. The input constraints of the UAVs are set as $12m/s \leq v_i \leq 25m/s$ and $|\omega_i| \leq 0.5rad/s$.

4.1 Formation Generation and Keeping

By employing the control law (6) with $G = 2$, the trajectories of six UAVs are shown in Fig.3. It is clear that the UAVs track the virtual leader whose path is represented by the green line. The corresponding distances between UAVs and their neighbors are shown in Fig.4(a), which implies that the distance converges to L. Besides, the corresponding distances between UAVs and the leader converge to $R = 40m$, as shown in Fig.4(b). Therefore, the standard formation depicted in Fig.1 is formed and kept.

As for the linear and angular speed constraints of fixed-wing UAVs, Fig.5(a) and Fig.5(b) show that v_i and ω_i are bounded by $v_{\min}$, $v_{\max}$ and $\omega_{\max}$, meaning the proposed control law is effective even with control input constraints.

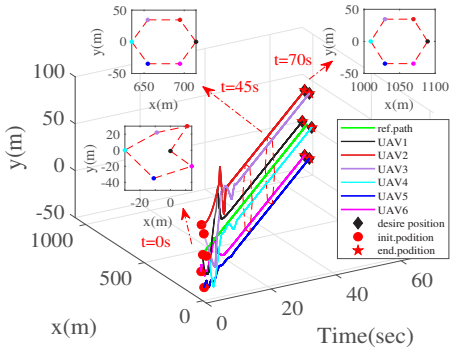

Fig. 3: The trajectories of six fixed-wing UAVs. UAVs track the virtual leader and converge to the standard formation.

4.2 Obstacle Avoidance

To demonstrate the virtual repulsion strategy, we add two obstacles in the simulations, and their parameters are shown in the Table 1. In the presence of obstacles, the position of

Table 1: Parameters of Virtual Repulsion f_{obs}

	Position	R_{obs}	L_{obs}
Obstacle 1	(900, 42)	10	20
Obstacle 2	(580, -6)	20	50

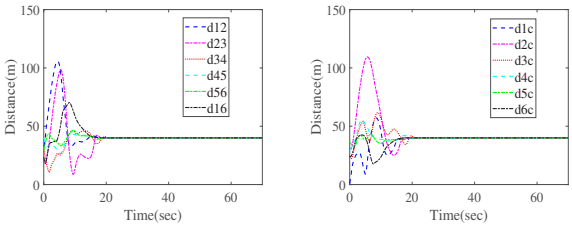

(a) The distance between UAVs and their neighbors, i.e., L.

(b) The distance between UAVs and the virtual leader,i.e., R.

Fig. 4: The variation of L and R.

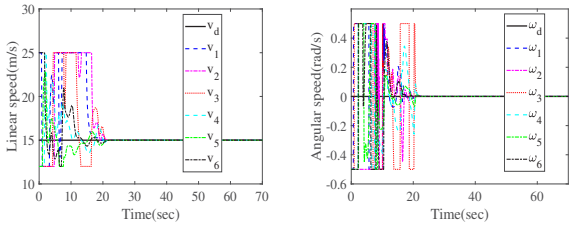

(a) The linear speeds, v_i.

(b) The angular speeds, ω_i.

Fig. 5: The variation of linear speeds and angular speeds.

UAVs during maneuvering is shown in Fig.6. Fig.7(a) and Fig.8(a) are partial enlarged views of Fig.6 to show the simulations more clearly. It is obvious that there are no collisions between UAVs and obstacles. Moreover, the repulsion increases as the distance between UAVs and the obstacles decreases, as shown in Fig.7(b) and Fig.8(b).

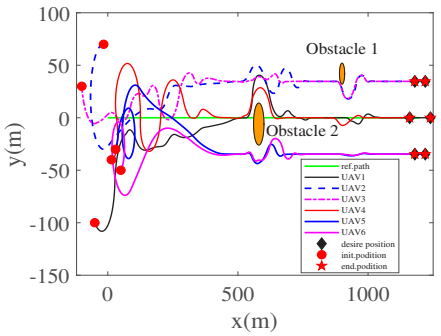

Fig. 6: The trajectories of six fixed-wing UAVs in the presence of obstacles. UAVs converge to the standard formation and avoid obstacles.

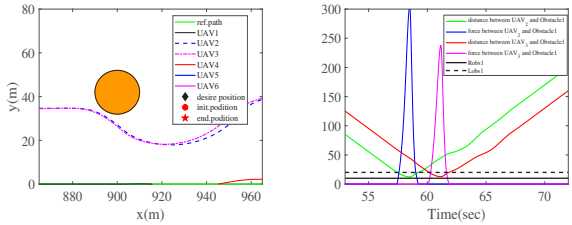

(a) The enlarged view of Obstacle 1 in Fig.6.

(b) The distance and repulsion between UAV_2/UAV_3 and Obstacle 1.

Fig. 7: The variation of distance and repulsion between UAVs and Obstacle 1 during flight. UAVs avoid collision with obstacles successfully.

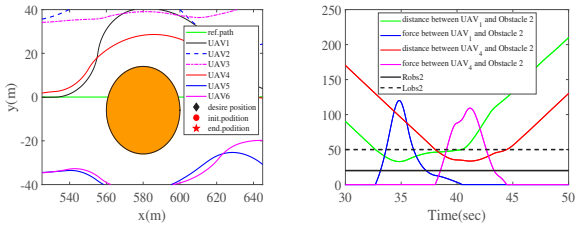

(a) The enlarged view of Obstacle 2 in Fig.6.

(b) The distance and repulsion between UAV_1/UAV_4 and Obstacle 2.

Fig. 8: The variation of distance and repulsion between UAVs and Obstacle 2 during flight. UAVs avoid collision with obstacles successfully.

5 Conclusion

This paper proposes a novel distributed formation control law for multiple fixed-wing UAVs. For a given standard formation, we define a potential function to measure the deviation between current position and target position. Control law is proposed based on the gradient of the potential function. To avoid collisions with possible obstacles during the flight, we propose the virtual repulsion strategy. Simulations are provided, showing that under the proposed control strategy, the UAVs can successfully form the desired formation and avoid obstacles. Stability analysis in the presence of input constraints is our future research direction.

References

[1] X. Wang, Z. Zeng, and Y. Cong, Multi-agent distributed coordination control: Developments and directions via graph viewpoint, *Neurocomputing*, 199: 204–218, 2016.

[2] K. K. Oh, M. C. Park, and H. S. Ahn, A survey of multi-agent formation control, *Automatica*, 53: 424–440, 2015.

[3] Y. Cao, W. Yu, W. Ren, et al, An overview of recent progress in the study of distributed multi-agent coordination, *IEEE Transactions on Industrial informatics*, 9(1): 427–438, 2013.

[4] H. G. Tanner, G. J. Pappas, and V. Kumar, Leader-to-formation stability, *IEEE Transactions on Robotics and Automation*, 20(3): 443–455, 2004.

[5] Z. Miao, Y. Liu, Y. Wang, et al, Distributed estimation and control for leader-following formations of nonholonomic mobile robots, *IEEE Transactions on Automation Science and Engineering*, 15(4): 1946–1954, 2018.

[6] W. Zhao, W. Yu, and H. Zhang, Observer-based formation tracking control for leader-follower multi-agent systems, *IET Control Theory and Applications*, 13(2): 239–247, 2019.

[7] Z. Sun, Y. Xia, Receding horizon tracking control of unicycle-type robots based on virtual structure, *International Journal of Robust and Nonlinear Control*, 26(17): 3900–3918, 2016.

[8] T. Balch, R. C. Arkin, Behavior-based formation control for multirobot teams, *IEEE Transactions on Robotics and Automation*, 14(6): 926–939, 1998.

[9] G. Antonelli, F. Arrichiello, and S. Chiaverini, Flocking for multi-robot systems via the null-space-based behavioral control, *Swarm Intelligence*, 4(1): 37–56, 2010.

[10] V. Gazi, Swarm aggregations using artificial potentials and sliding-mode control, *IEEE Transactions on Robotics*, 21(6): 1208–1214, 2005.

[11] H. Hu, S. Y. Yoon, and Z. Li, Coordinated control of wheeled vehicles in the presence of a large communication delay through a potential functional approach, *IEEE Transactions on Intelligent Transportation Systems*, 15(5): 2261–2272, 2014.

[12] C. Kownacki, L. Ambroziak, Local and asymmetrical potential field approach to leader tracking problem in rigid formations of fixed-wing UAVs, *Aerospace Science and Technology*, 68: 465–474, 2017.

[13] O. Khatib, Real-time obstacle avoidance for manipulators and mobile robots, in *Proceedings of 1985 IEEE International Conference on Robotics and Automation*, 1985: 90–98.

[14] W. Spears, D. Gordon, Using artificial physics to control agents, in *Proceedings of 1999 International Conference on Information Intelligence and Systems*, 1999: 281–288.

[15] X. Wang, X. Wang, D. Zhang, et al, A liquid sphere-inspired physicomimetics approach for multiagent formation control, *International Journal of Robust and Nonlinear Control*, 28(15): 4565–4583, 2018.

[16] L. Shen, X. Wang, H. Zhu, Y. Fu, et al, UAVs flocking and reconfiguration control based on artificial physics(in Chinese), *Scientia Sinica Technologica*, 47: 266–285, 2017.

[17] H. Chen, Y. Cong, X. Wang, et al, Coordinated path following control of fixed-wing unmanned aerial vehicles, arXiv preprint arXiv:1906.05453, 2019.

[18] X. Wang, L. Shen, Z. Liu, et al, Coordinated flight control of miniature fixed-wing UAV swarms: methods and experiments, *Science China Information Sciences*, 62(11): 212204.